López-Hernández, I.; Truttmann, V.; Barrabés, N.; Rupprechter, G.; Rey Garcia, F.; Mengual Cuquerella, J.; Palomares Gimeno, AE. (2022). Gold nanoclusters supported on different materials as catalysts for the selective alkyne semihydrogenation. Catalysis Today. 394:34-40. https://doi.org/10.1016/j.cattod.2022.02.014

Catalysis Today

Gold nanoclusters supported on different materials as catalysts for the selective alkyne semihydrogenation

--Manuscript Draft--

Manuscript Number:	
Article Type:	SI:CICAT2020
Keywords:	alkynes; gold nanoclusters; selective hydrogenation; support; hydrotalcite
Corresponding Author:	Antonio Eduardo Palomares, PhD Universidad Politecnica Valencia Valencia, SPAIN
First Author:	Antonio Eduardo Palomares, PhD
Order of Authors:	Antonio Eduardo Palomares, PhD
	Irene Lopez-Hernandez
	Vera Truttmann
	Noelia Barrabes
	Günther Rupprechter
	Fernando Rey
	Jesus Mengual
Abstract:	Catalysts based on gold nanoclusters supported by different materials have been used for the selective semihydrogenation of phenylacetylene to styrene. The most active species were formed by catalyst thermal activation in a reductive atmosphere. It is shown that the activity and selectivity of these catalysts is mainly controlled by the interaction of the gold nanoclusters with the support, as demonstrated by using materials with high surface area and different acidity/basicity, i.e. MgO, Al_2O_3 and Mg/Al hydrotalcite. There is an important influence of the acid/base properties of the support on the selectivity. Higher activity is obtained for gold supported on basic materialss (MgO and hydrotalcite) and the best results are obtained with the Au catalyst supported on the MgAl hydrotalcite exhibiting high activity and the best selectivity to the alkene. This was explained by the intermediate basicity of the support that favors the heterolytic cleavage of H_2 while avoiding the overreduction of the alkynes to alkanes.
Suggested Reviewers:	Julia Aguilar Universidad Autónoma Metropolitana: Universidad Autonoma Metropolitana apj@azc.uam.mx
	Katia Gusman Universidade Federal do Rio Grande do Sul katia.gusmao@ufrgs.br
	Geolar Fetter Benemerita Universidad Autonoma de Puebla geolarfetter@yahoo.com.mx
	Hannu Häkkinen Jyvaskylan Yliopisto hannu.j.hakkinen@jyu.fi
	Tatsuya Tsukuda University of Tokyo: Tokyo Daigaku tsukuda@chem.s.u-tokyo.ac.jp

Catalysis Today Editor

Valencia, 9 April 2021

Dear Sir,

Please find enclosed the manuscript entitled:
"Gold nanoclusters supported on different materials as catalysts for the selective alkyne semihydrogenation" by I. López-Hernández, V. Truttmann, N. Barrabés, G. Rupprechter, J. Mengual, F. Rey and A. E. Palomares in order to be considered for a possible publication in your journal.
This paper studies the influence of the support and the gold nanocluster activation on the activity of the catalyst for the selective semihydrogenation of alkynes. The results obtained evidenced the influence of the acid/base properties of the support on the catalyst activity and it is shown that the optimum catalyst must be prepared by a delicate balance among basicity, stability of gold nanoparticles and accessibility to the reactants. It is shown that the best catalytic results in the hydrogenation of phenylacetylene to styrene are obtained with a gold nanocluster pretreated with H_2 and supported on a material with an intermediate basicity i.e. Mg/Al hydrotalcite. This contribution was presented by one of the authors (I. López-Hernández) as an oral contribution in the CICAT 2020. We believe that this contribution is suitable for the scope of this journal covering both fundamental and applied aspects of catalysis and that it is of great interest for the scientific community. We also apologize for the delay in sending the paper but we confuse the deadline and hope that we are still in time for considering this contribution.

With my best regards:

Dr. A.E. Palomares

Instituto Tecnología Química
Universidad Politécnica de Valencia-CSIC
Camino de Vera s.n.
46022-Valencia
(Spain)
apalomar@iqn.upv.es
tel. +34963877007 ext. 76377

XXVII
CONGRESO
IBEROAMERICANO
DE CATÁLISIS 2020
México

Official CICAT 2020 Invitation letter

Dear AnTOnio Eduardo Palomares, Fernando Rey, Irene López, Noelia Barrabés, Clara Yago, Vera Truttmann, Stephan Pollitt and Guenther Rupprechter we are pleased to inform you that the Scientific Committee of the XXVII Congreso Iberoamericano de Catálisis has selected your congress contribution:# 63, "ESTUDIO DE LA NATURALEZA DE LAS ESPECIES DE PLATA PRESENTES EN CATALIZADORES MEDIANTE LA OXIDACIÓN CATALÍTICA DE CO" for possible publication in the Special Issue of the ***Catalysis Today*** Elsevier Journal.

The submission period will be from 4th January to 19th February. The deadline to submit your work to the editorial manager is February 19th, 2021. Pay Attention that there will be **no extension** of this day. Also, be aware that this invitation does not guarantee the publication of your manuscript. The final decision of acceptance or rejection will be made on the basis of the peer review evaluations on Elsevier´s platform.

Please read the Guide for authors at https://www.elsevier.com/journals/catalysis-today/0920-5861/guide-for-authors and follow all recommendations prior to submitting your manuscript.

To submit your paper, follow the next instruction

Select SI: CICAT2020 in the article type menu.

Select **Guest Editor** as managing editor in the request editor menu

Remember to upload this official invitation letter.

J. N. Díaz de León
Guest Editor

S. Fuentes-Moyado
Guest Editor

G. Alonso-Nuñez
Guest Editor

T.A. Zepeda-Partida
Guest Editor

Highlights:

- Supported Au-nanoclusters are active catalysts for the alkyne semihydrogenation.

- Activity depends on the pretreatment and on the acidity/basicity of the support

- Most active gold species were formed by thermal activation in a reductive atmosphere

- Au-catalysts supported on basic oxides are more active than supported on acidic ones

- Best results were obtained with Au_{25} clusters supported on a MgAl hydrotalcite

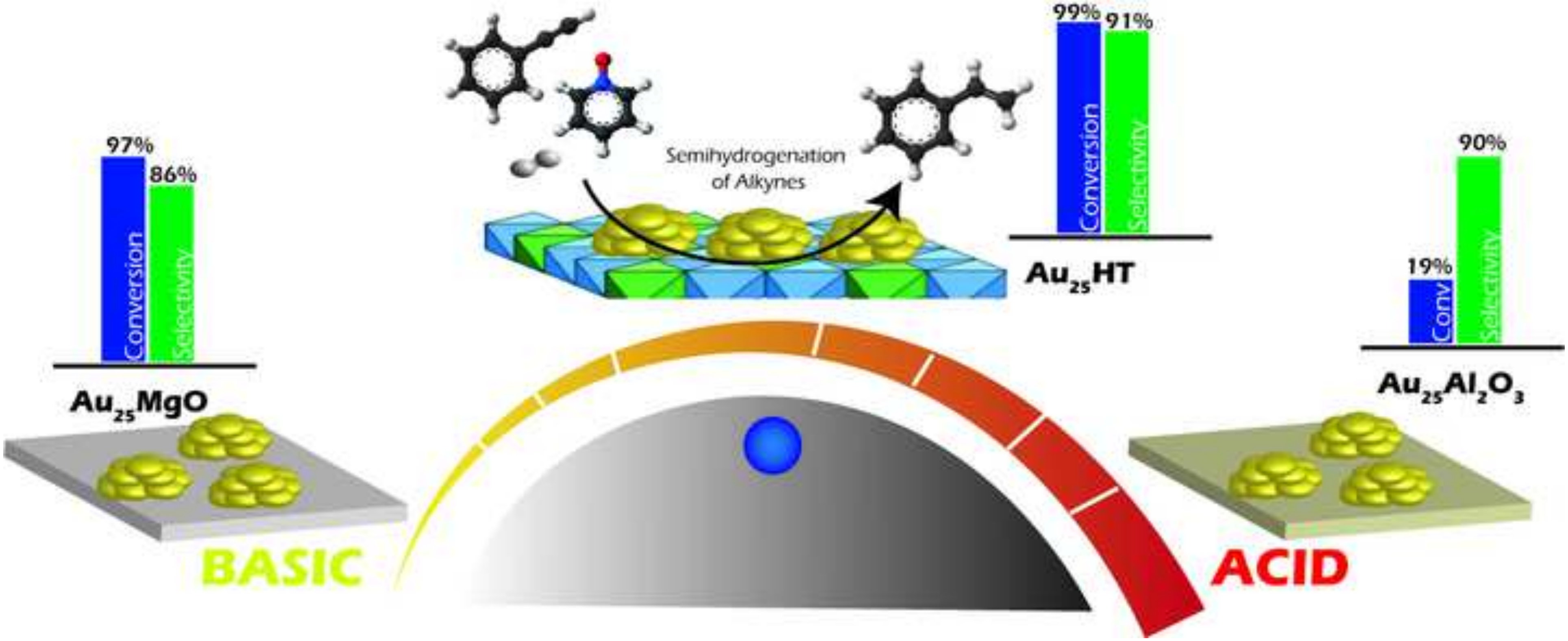
97%
86%
Conversion
Selectivity
Au25MgO
BASIC
Semihydrogenation of Alkynes
99%
91%
Conversion
Selectivity
Au25HT
19%
90%
Conv
Selectivity
Au25Al2O3
ACID

Gold nanoclusters supported on different materials as catalysts for the selective alkyne semihydrogenation

I. López-Hernández[1], V. Truttmann[2], N. Barrabés[2,*], G. Rupprechter[2], F. Rey[1], J. Mengual[1], A. E. Palomares[1,*]
[1]*Instituto de Tecnología Química, Universitat Politècnica de València - Consejo Superior de Investigaciones Científicas (UPV-CSIC), Valencia, España*
[2]*Institute of Materials Chemistry, TU Wien, Vienna, Austria*

Corresponding author: apalomar@iqn.upv.es, noelia.rabanal@tuwien.ac.at

Keywords: alkynes, gold nanoclusters, selective hydrogenation, support, hydrotalcite

Abstract

Catalysts based on gold nanoclusters supported by different materials have been used for the selective semihydrogenation of phenylacetylene to styrene. The most active species were formed by catalyst thermal activation in a reductive atmosphere. It is shown that the activity and selectivity of these catalysts is mainly controlled by the interaction of the gold nanoclusters with the support, as demonstrated by using materials with high surface area and different acidity/basicity, i.e. MgO, Al_2O_3 and Mg/Al hydrotalcite. There is an important influence of the acid/base properties of the support on the selectivity. Higher activity is obtained for gold supported on basic materialss (MgO and hydrotalcite) and the best results are obtained with the Au catalyst supported on the MgAl hydrotalcite exhibiting high activity and the best selectivity to the alkene. This was explained by the intermediate basicity of the support that favors the heterolytic cleavage of H_2 while avoiding the overreduction of the alkynes to alkanes.

1. Introduction

Catalytic hydrogenation is a key process technology in the petrochemical and pharmaceutical industry. Around 25% of all chemical processes include, at least, a catalytic hydrogenation step [1,2]. These reactions usually occur through the activation of molecular hydrogen *via* its homolytic dissociation on a noble metal surface, such as Pt, Pd and Rh [3]. Nevertheless, in order to obtain more sustainable processes, new catalysts are necessary [3].

Among the different catalytic hydrogenation reactions, semihydrogenation of alkynes has been a focus of attention due to its relevance in the manufacturing of fine chemical and polymers [4,5]. Selective semihydrogenation of alkynes can be carried out using different active metals, such as palladium [6–8], iridium [9], ruthenium [10,11], iron [12] and nickel [5]. Metallic gold is also attracting some interest due to its excellent catalytic performance in hydrogenation processes [13–15]. In this context, the use of gold nanoparticles for catalysing these reactions has been described, reporting exceptional selectivity and high activity [16–18]. Yan *et al*. reported the use of unsupported nanoporous gold for the selective semihydrogenation of alkynes using organosilanes with water as a hydrogen source. They suggested that the metallic Au(0) species were the catalytic active sites for the reaction [19]. Gold nanoparticles supported on oxides such as TiO_2 have also been employed in selective hydrogenation of quinoline with H_2 reporting good results under mild reaction conditions [14].

In order to understand the correlation of the activity and selectivity with structural properties of the catalysts, the use of small metal clusters has been proposed [20]. This rather new class of nanomaterials can be obtained with atomic precision, with a unique well-defined molecular structure and intriguing molecular-like properties. Due to these characteristics combined with small particle sizes, lower than 2 nm, nanoclusters exhibit activity for several catalytic reactions. Gold nanoclusters have been tested in different catalytic hydrogenation reactions such as the chemoselective hydrogenation of α, β-unsaturated aldehydes and ketones [21], the reduction of 4-nitrophenol by $NaBH_4$ [22,23], the chemoselective hydrogenation of nitrobenzaldehyde into alcohols [24] or the selective hydrogenation of terminal alkynes to alkanes using H_2 [25].

In this context, the selective semihydrogenation of alkynes using gold nanoclusters catalysts is attracting much interest as the reductive ability of gold is lower than that of Pt or Pd. These noble metals are usually employed to catalyse this reaction but they must be partially poisoned to avoid over-reduction of alkynes, wasting an important part of these valuable materials. Thus, the use of gold nanoclusters as catalyst for this reaction may be a more sustainable approach in line with the Green Chemistry Principles [26]. In the selective semihydrogenation of alkynes, selectivity is one of the most important objectives to be achieved, avoiding reduction of alkynes to non-valuable alkanes [27]. It has been described [15,25] that selectivity and activity of gold nanoparticles for this reaction can be improved by adding base molecules to the reaction media. The best results have been obtained with nitrogen-containing molecules as they form frustrated Lewis pair interfaces that activate H_2 heterolytically, increasing the hydrogenation activity.

The nature of supports should also affect the activation of H_2, as it occurs in other hydrogenation reactions [28]. Nevertheless, Jin *et al.* did not observe an obvious influence on the catalytic performance of gold nanoclusters supported on SiO_2, Al_2O_3, CeO_2 and TiO_2 [25] used for the semihydrogenation of terminal alkynes. On the other hand, different results were obtained by Rossi *et al.* [15], obtaining the best catalytic performance in the hydrogenation of phenylacetylene with gold nanoparticles supported on TiO_2 and SiO_2, while those supported on CeO_2 were less active and those supported on Al_2O_3 were less selective.

Within this work, we studied the use of gold nanoclusters supported on various materials with high surface area and different acid/base properties for the selective hydrogenation of phenylacetylene to styrene. The supports used are alumina that has acid properties, MgO with basic properties and Mg/Al hydrotalcite that is a layered material with an intermediate basicity. The influences of the nanocluster size, the characteristics of the support and the activation procedure on the catalyst activity and selectivity are discussed and the catalytic results are correlated with the acid/base properties of the material.

2. Experimental

2.1. Catalyst preparation

Synthesis of $Au_{25}(SC_2H_4Ph)_{18}$ nanoclusters, (Au_{25}), was made following the protocol described by Shivhare *et al.* [22]. According to it 1.27 mmol of $HAuCl_4{\cdot}3H_2O$ were dissolved in 50 mL of tetrahydrofuran (THF) and the obtained solution was mixed with 1.2 equivalents of tetraoctylammonium bromide (TOAB) and stirred for 10 minutes.

Then, 5 equivalents of the thiol-ligand (2-phenylethanethiol) were added dropwise, and the solution was stirring until becomes transparent. After that, 10 equivalents of $NaBH_4$ were dissolved in 10 mL of ice-cold water and added to the solution as a reducing agent. The solution was stirred for 4 days. Finally, the solvent was evaporated and the residue was washed with mixtures of ethanol/water. The nanoclusters were extracted with THF and separated by size-exclusion chromatography.

The synthesis of $Au_{11}(PPh_3)_7Br_3$ nanoclusters (Au_{11}) was carried out according to [29] and 1.27 mmol of $HAuCl_4·3H_2O$ and 1.2 equivalents of TOAB were dissolved in 50 mL of THF. After that, 5 equivalents of PPh_3 were added and the solution was stirred for 1 hour. Then, 10 equivalents of $NaBH_4$ were dissolved in 10 mL of ice-cold, and this was added to the previous solution. This solution was stirred during 48 hours forming a precipitate. The solvent was removed by evaporation and the solid was washed several times with 1:1 mixtures of methanol:water. The by-products were extracted with THF, toluene and 2:1 mixture of hexane:ethanol. Finally, the Au_{11} nanoclusters were extracted with dichloromethane (DCM).

The materials used to support the gold nanoclusters were MgO, Mg/Al hydrotalcite and Al_2O_3. Alumina was supplied by abcr GmbH. High surface area MgO was synthesized according to [30] and 25 g of $(MgCO_3)_4Mg(OH)_2$ were suspended in 750 mL of water and stirred at 80ºC for 30 minutes, the solid was filtered and dried at 90ºC during 24 hours, and then calcined at 450ºC for 2 hours. Mg/Al hydrotalcite was prepared by the co-precipitation method. According to it, an acidic solution containing $Mg(NO_3)_2$ and $Al(NO_3)_3$ was mixed with a basic one containing NaOH and $NaNO_3$. The amount of each reactive was chosen to obtain a molar ratio of Mg/Al = 4. Both solutions were mixed (room temperature and atmospheric pressure) dropwise using an infusion pump ($1\ mL·min^{-1}$) while stirring the resulting solution. The solution was aged at 60ºC for 24 hours and the solid was filtered and washed several times with water until pH=7. Finally, the solid was dried at 100ºC during 24 hours.

The Au_{25} and Au_{11} nanoclusters were supported on the oxides and on the hydrotalcite by solving the nanocluster in toluene and adding the supports to the solution that was stirred during 24 hours. The samples were centrifuged and separated by decantation. The catalysts were dried at 80ºC for 1 hour.

2.2. Catalytic tests

The catalytic test was performed in a reinforced glass reactor equipped with temperature and pressure control. 0.1 mmol of phenylacetylene and 0.2 mmol of pyridine (as base molecule) were diluted in 1 mL of solvent (EtOH:H_2O 10:1 V/V) and were placed into the reactor (8 mL capacity) together with an appropriate amount of catalyst (100 mg). After sealing the reactor, air was purged by flushing two times with 10 bar of hydrogen. Then, the autoclave was heated to the required temperature (100ºC) and finally the pressure (10 bars) was adjusted with H_2. The stirring rate was fixed at 1000 rpm. The reaction was made at 100 ºC for 20 h. After reaction, the solution was filtered and analysed by gas chromatography, using a Varian CP-3800 analyser equipped with a split/splitless injector and a HP-5 column of 25 m length (0.25 mm of i.d. and 0.25 μm active phase thickness). The products were detected using a flame ionization detector (FID). The relative response factors, which allow the calculation of the corrected area for phenylacetylene, styrene and ethylbenzene, were determined from a calibration obtained from different ternary mixtures. From the values of the corrected areas (A_{C_j}), total conversion (X), mass fractions (w_j) and selectivity (S_{mas_j}) were calculated according to the following equations:

$$w_j(\%) = \frac{A_{C_j}}{\sum_j^3 A_{C_j}} \cdot 100 \tag{1}$$

$$X(\%) = 100 - w_{FA}(\%) \tag{2}$$

$$S_{mas_j}(\%) = \frac{w_j(\%)}{X(\%)} \cdot 100 \tag{3}$$

where w_{FA} is the mass fraction of the phenylacetylene at the end of the hydrogenation reaction.

2.3 Characterization studies

Temperature programmed reduction with H_2 (H_2-TPR) was performed in a TPD-TPR Autochem 2910 equipment connected to a thermal conductivity detector (TCD). Prior to the reduction, samples were treated under Ar flow during 1 hour at room temperature. During the TPR analysis, a mix of 10% H_2 in Ar was used while the temperature was increased from room temperature to 600ºC with a ramp of 10ºC/min.

UV-Vis DRS measurements were performed on a Varian Cary 5000 spectrophotometer equipped with a diffuse reflectance attachment, and the spectra were recorded at room temperature in the wavelength range from 200 to 800 nm.

N_2 adsorption isotherms were measured at −196 °C in ASAP-2420 equipment (Micromeritics). Surface areas of the catalysts were obtained by the BET method (S_{BET}).

The chemical composition of the samples was measured by inductively coupled plasma in a Varian 715-ES ICP-Optical Emission Spectrometer.

Pyridine adsorption–desorption experiments were carried out using Nicolet iS10 FTIR spectrometer. The samples were previously activated overnight at 400ºC under vacuum. After activation, the reference spectrum was recorded and pyridine vapour was admitted in the cell and adsorbed onto the sample. The excess of pyridine was removed in vacuum by heating for 1 h at 150, 250, and 350ºC, respectively. After each heating period, the sample was cooled to room temperature and IR spectrum was recorded. All the spectra were scaled according to the sample weight.

3. Results and discussion

Gold nanoclusters with different number of atoms (Au_{25} or Au_{11}) were supported on materials with high surface area and different acid/base properties (MgO, Al_2O_3 and Mg/Al hydrotalcite) and their activity was studied for the selective hydrogenation of phenylacetylene to styrene in the presence of pyridine.

The XRD patterns of the different supports (Figure S1) show the characteristic peaks of the materials, i.e. the mean peaks assigned to MgO at 2θ = 37.0, 43.1 and 62.9°, the peaks characteristic of γ-Al_2O_3 at 2θ = 37.5, 39.5, 45.9, 61.0 and 66.9° and the peaks of a hydrotalcite phase at 2θ = 11.2, 22.7, 34.4, 38.4, 45.5, 46.7, 60.1, 61.8 and 65.3° for the Mg/Al hydrotalcite. The catalysts have a BET surface area around 100-225 m^2/g with type II isotherms typical of mesoporous materials. The chemical composition and the textural characteristics of the catalysts are shown in Table 1.

The influence on the catalytic activity of acid/base properties of the support and the number of gold atoms in the nanocluster were studied with the fresh Au_{11} and Au_{25} nanoclusters supported on MgO and Al_2O_3. Figure 1 shows the catalytic behaviour of the nanocluster catalysts in phenylacetylene hydrogenation, displaying the conversion and selectivity towards styrene (desired product) and ethylbenzene (side products) with pronounced support effect being evident. MgO supported catalysts lead to almost completed conversion of phenylacetylene, whereas lower activities are obtained with the gold catalysts supported on Al_2O_3. In the case of alumina supported catalysts, different activity depending on the gold cluster size is noted, obtaining conversions of almost 60% with Au_{11} versus 9% with Au_{25}. On the contrary, these differences are not observed for the catalysts supported on MgO. Magnesium oxide is a basic type support contrary to the acidic character of Al_2O_3, therefore an influence of the acid-base properties of the oxide support seems evident.

However, in addition to the distinct atom number also the type of ligand is different for Au_{11} and Au_{25} nanoclusters. Au_{25} has a thiolate ligand (SC_2H_4Ph), whereas Au_{11} has a phosphate one (PPh_3). Recently, for the semihydrogenation of alkynes, different catalytic performance depending on the type of ligand was observed on $[Au_{38}(L)_{20}Ph_3P_4]^{2+}$ (L=alkynil of thiolate) nanoclusters supported on TiO_2 [31]. As for our alumina samples, thiolate-protected Au_{38} catalyst exhibited lower activity than alkynil-protected catalysts. On the other hand, Jin *et al.* reported no influence on the type of ligand for $Au_{25}(SCH_4Ph)_{18}$ and $Au_{25}(PPh_3)_{10}(CCPh)_5Br_2$ supported on TiO_2 [25], as with our MgO samples. Moreover, it must be taken into account that due to the reaction conditions, the ligands will be partially decomposed during reaction and gold nanocluster will evolve towards the formation of gold nanoparticles. To avoid such changes and for a better understanding of the role of the supports, the current catalysts were thermally pretreated before reaction.

The influence of oxidative or reductive thermal pretreatments, i.e. in presence of hydrogen or air, on catalyst activity was first studied for the Au_{11} nanoclusters supported on alumina. Both pretreatments were performed at 300ºC as under these conditions, most of the ligands are removed. Figure 2 shows that the initial activity of the fresh catalyst is doubled after the oxidative or reductive pretreatments, but in both cases this goes along with a drop in selectivity. However, reductive pretreatment still has 33% selectivity towards styrene, while it is only 2% for the catalysts pretreated with air.

The catalytic results can be related to the changes of the nanocluster that occur during these pretreatments. The activation of the catalyst removes to some extent the ligands from the nanoclusters, allowing a better interaction of the reactants with the gold active sites, i.e. the triple bond interacts directly with the gold nanocluster surface. Thus, a higher conversion is expected. The same pretreatment effect occurs for other reactions, e.g. CO oxidation on silver nanoclusters [32]. The evolution of the gold nanocluster during activation was studied by UV-Vis spectroscopy, yielding fingerprints of the cluster structure [33]. By comparing pure cluster in solution with supported one and after each pretreatment (Figure 3), information on the nanocluster stability was obtained. The spectrum of unsupported Au_{11} nanoclusters (Figure S2) shows a characteristic peak at 420 nm indicating quantized electronic structure [34]. The diffuse reflectance UV-vis spectrum of the alumina supported $Au_{11,}$ as seen in Figure 3, also shows this characteristic band. Nevertheless, after the thermal treatments the band disappears, forming an intense and broad band at 530-550 nm that may be related to agglomeration of the clusters on the oxide surface after the ligand removal.

The differences in the selectivity of the catalyst pretreated with H_2 and air may be related to the formation of smaller gold nanoparticles for the first [35], as well as to the reduction of oxidized species coexisting in the catalyst [36]. Moreover, during the oxidative pretreatment, ligands are more efficiently removed resulting in an increased exposure of gold sites that may lead to an overreduction of the phenylacetylene to ethylbenzene.

The results obtained in this reaction with the fresh nanoclusters and previous reported results with gold nanoclusters in other reactions [37,38], have shown a strong effect of support properties on the catalytic behaviour of nanocluster catalysts. Accordingly, the influence of the support in the catalytic semihydrogenation of phenylacetlyne in presence of pyridine was further studied with catalysts pretreated with hydrogen at 300ºC. This study was made with gold nanocluster catalysts supported on two different materials, one with basic (MgO) and another one with acidic properties (Al_2O_3). As Figure 4 (left and middle) shows, the level of activity is not affected, whereas a pronounced effect on selectivity is observed. Au_{11} supported on a basic material as MgO leads to 59% styrene selectivity, while 33% is obtained with the same nanoclusters supported on the more acid Al_2O_3. Again, the acid/base properties of the support are playing an important role in the reaction pathway, as already observed with the fresh catalysts. This may be related to the electronic properties of the support that directly affect the adsorption strength of the reactants to the metal surface, thus influencing activity and selectivity.

The limiting step in hydrogenation reactions used to be the activation of H_2. It has been reported that when using gold nanoparticles as catalysts for this reaction, the H_2 activation is favoured by the addition of N-containing basic molecules to reaction media [15]. The coadsorption of these basic molecules increases the activity and selectivity of gold catalyst in the alkyne semihydrogenation reaction. This is explained by the formation of frustrated Lewis pair between gold nanoparticles and the N-containing basic molecules that activates H_2 heterolytically [15]. The activated hydrogen then reacts with the adsorbed alkyne forming the alkene. Thus, the H_2 dissociation depends on the Au–basic molecule interaction. A strong interaction could activate too much the H_2 and could arrive to trigger metal extraction, while a weak interaction does not form a frustrated Lewis pair and consequently hydrogen is not activated. Thus, the basicity of the N-base molecules, as well as the acid-base properties of the catalyst surface determine the interaction. Pyridine is used in these experiments as the N-containing basic molecule but it is a strong basic molecule that may cause gold extraction if the interaction gold-pyridine is strong enough [15]. It is expected that this interaction is favoured with gold on acidic surfaces, however if gold is supported on a basic material the interaction of the basic molecule with the basic surface will be modulated and the frustrated Lewis pairs will be formed on the catalyst surface, activating the H_2 but avoiding the overreduction of the alkyne. This may explain the higher selectivity towards styrene for gold catalyst support on MgO as compared to the more acidic Al_2O_3.

At this point, using MgO as support and reductive pretreatment appear as being optimal. Therefore, the performance of Au_{25} was also studied for these conditions (Figure 4 right). Similar conversion levels as with Au_{11}/MgO catalysts were obtained, but a remarkable increase in styrene selectivity toward styrene was achieved, likely related to the higher stability of Au_{25} nanoclusters upon reductive pretreatment. UV-Vis spectra of both catalysts after pretreatment are shown in Figure 5. The main difference in both spectra is the band at 526 nm assigned to gold nanoparticles. This band is observed for the Au_{11} catalyst denoting the sintering of gold nanoclusters, whilst it does not appear in the spectrum of Au_{25} catalysts indicating a higher stability of gold nanoclusters in this catalyst.

Finally a Mg/Al hydrotalcite (HT) support with a basicity intermediate between MgO and Al_2O_3 was impregnated with the Au_{25} nanoclusters. Hydrotalcites are layered materials that can be prepared with different divalent and trivalent metals and that are used as supports or catalysts in many reactions [39–41]. The activity of the catalyst supported on the hydrotalcite (with a Mg:Al molar ratio of 4) was compared with Au_{25} on Al_2O_3 and MgO activated in a reductive atmosphere (Figure 6). Au_{25} supported on the acidic alumina support is the less active, whilst those supported on basic materials, i.e. MgO and Mg/Al hydrotalcite are much more active. As previously discussed, this may be related with a lower interaction of the pyridine with gold supported on the basic materials that results in a better activation of H_2. Thus, pyridine adsorption-desorption was followed by infrared spectroscopy. As seen in Figure 7, pyridine mainly adsorbs on the three catalysts through the Lewis acid sites characterized by the band around 1450 cm^{-1}. As expected, the area of this band is higher for the more acidic catalyst, i.e. the alumina supported, indicating a higher number of acid sites. These sites interact more strongly with the pyridine than the Lewis sites of MgO or hydrotalcite as the intensity of the bands are higher at 250-350ºC for the alumina supported catalyst. As it was previously discussed, the weaker interaction of the pyridine with the surface of more basic catalysts favours the formation of frustrated Lewis pairs that activates H_2 heterolytically, increasing the activity of the catalysts.

Comparing the selectivity of the catalysts supported on basic materials, i.e., MgO and Mg/Al hydrotalcite, somewhat higher styrene selectivity (91%) is obtained with the Au_{25}/HT. This suggests hydrotalcite as optimal support for gold nanocluster catalysts in this reaction, showing higher activity and selectivity than the Al_2O_3 and MgO supported ones. It was proposed [35,42,43] that a concerted effect exists between the basic sites of hydrotalcite and the Au-nanoparticles favouring the heterolytic cleavage of H_2, producing Au-hydride and H^+ on the hydrotalcite surface. These hydrogen species react with the adsorbed alkyne forming the alkene. This effect is similar to the one produced by pyridine, but with the advantage that Au/HT is inactive for the hydrogenation of C=C bonds [35,42], improving the selectivity of the reaction.

The interaction of hydrogen with the catalsyts surface was evaluated by TPR. Figure 8 compares the TPR profile of the three pre-oxidized catalysts. The thermogram of the MgO supported catalyst is dominated by an intense well-defined peak centered at 327ºC. In the case of the hydrotalcite supported catalyst, an intense broader peak is around 388°C and for the alumina catalyst no clear peaks are obtained. This indicates that the reducible species in Au_{25}/MgO, interact more easily with hydrogen than in Au_{25}/HT, whilst almost no interaction of hydrogen with the alumina supported catalyst is observed. This may be related to the basic characteristics of the supports, that as the pyridine does, favours the activation of hydrogen leading to a higher activity of the catalysts. However a strong activation of the H_2 may also result in overreduction of the alkene, explaining why supports with intermediate basicity such as hydrotalcites lead to better alkenes selectivity.

CONCLUSIONS

Supported gold nanoclusters are active catalysts for the selective hydrogenation of phenylacetylene to styrene. The activity depends on the pretreatment and on the acid/base characteristics of the support. For Au_{25} better selectivity was achieved after a reductive pretreatment, probably because gold nanoparticles of smaller size are formed. Best results in terms of conversions and selectivity were obtained with Au_{25} clusters supported on a MgAl hydrotalcite that exhibits an intermediate basicity between MgO and Al_2O_3. The presence of these weaker basic sites favors the heterolytic cleavage of H_2 while avoiding the overreduction of the alkynes to alkanes. The results indicate that the optimum catalyst is created by a delicate balance among basicity, stability of gold nanoparticles and accessibility to the reactants.

Acknowledgements

The authors thank the Spanish Ministry of Economy and Competitiveness through RTI2018-101784-B-I00 (MINECO/FEDER) and SEV-2016-0683 projects for the financial support. I. López Hernández is grateful to Generalitat Valenciana and European Social Fund for the pre doctoral grant ACIF2017. We acknowledge support by the Austrian Science Fund (FWF) via Single Atom Catalysis (I 4434-N) and Elise Richter (V831-N).

4. References

[1] S. Nishimura, Handbook of Heterogeneous Catalytic Hydrogenation for Organic Synthesis, Wiley, New York, 2001. https://doi.org/10.1021/op0100798.

[2] R.A. Sheldon, H. van Bekkum, Fine Chemicals through Heterogeneous Catalysis, first edition, Wiley, Weinheim, 2001.

[3] G. Vilé, D. Albani, N. Almora-Barrios, N. López, J. Pérez-Ramírez, Advances in the Design of Nanostructured Catalysts for Selective Hydrogenation, ChemCatChem. 8 (2016) 21–33. https://doi.org/10.1002/cctc.201501269.

[4] S. Carenco, X.F. Le Goff, J. Shi, L. Roiban, O. Ersen, C. Boissière, C. Sanchez, N. Mézailles, Magnetic core-shell nanoparticles from nanoscale-induced phase

segregation, Chem. Mater. 23 (2011) 2270–2277. https://doi.org/10.1021/cm200575g.

[5] S. Carenco, A. Leyva-Pérez, P. Concepción, C. Boissire, N. Mézailles, C. Sanchez, A. Corma, Nickel phosphide nanocatalysts for the chemoselective hydrogenation of alkynes, Nano Today. 7 (2012) 21–28. https://doi.org/10.1016/j.nantod.2011.12.003.

[6] J. Li, R. Hua, T. Liu, Highly chemo- and stereoselective palladium-catalyzed transfer semihydrogenation of internal alkynes affording cis -alkenes, J. Org. Chem. 75 (2010) 2966–2970. https://doi.org/10.1021/jo100247a.

[7] R. Shen, T. Chen, Y. Zhao, R. Qiu, Y. Zhou, S. Yin, X. Wang, M. Goto, L.B. Han, Facile regio- and stereoselective hydrometalation of alkynes with a combination of carboxylic acids and group 10 transition metal complexes: Selective hydrogenation of alkynes with formic acid, J. Am. Chem. Soc. 133 (2011) 17037–17044. https://doi.org/10.1021/ja2069246.

[8] T. Mitsudome, Y. Takahashi, S. Ichikawa, T. Mizugaki, K. Jitsukawa, K. Kaneda, Metal-ligand core-shell nanocomposite catalysts for the selective semihydrogenation of alkynes, Angew. Chemie - Int. Ed. 52 (2013) 1481–1485. https://doi.org/10.1002/anie.201207845.

[9] K. Tani, A. Iseki, T. Yamagata, Efficient transfer hydrogenation of alkynes and alkenes with methanol catalysed by hydrido(methoxo)iridium(III) complexes, Chem. Commun. (1999) 1821–1822. https://doi.org/10.1039/a905765j.

[10] C. Belger, N.M. Neisius, B. Plietker, A selective Ru-catalyzed semireduction of alkynes to Z olefins under transfer-hydrogenation conditions, Chem. - A Eur. J. 16 (2010) 12214–12220. https://doi.org/10.1002/chem.201001143.

[11] J. Li, R. Hua, Stereodivergent ruthenium-catalyzed transfer semihydrogenation of diaryl alkynes, Chem. - A Eur. J. 17 (2011) 8462–8465. https://doi.org/10.1002/chem.201003662.

[12] C. Belger, B. Plietker, Aryl-aryl interactions as directing motifs in the stereodivergent iron-catalyzed hydrosilylation of internal alkynes, Chem. Commun. 48 (2012) 5419–5421. https://doi.org/10.1039/c2cc31395b.

[13] A. Arcadi, Alternative synthetic methods through new developments in catalysis by gold, Chem. Rev. 108 (2008) 3266–3325. https://doi.org/10.1021/cr068435d.

[14] D. Ren, L. He, L. Yu, R.S. Ding, Y.M. Liu, Y. Cao, H.Y. He, K.N. Fan, An unusual chemoselective hydrogenation of quinoline compounds using supported gold catalysts, J. Am. Chem. Soc. 134 (2012) 17592–17598. https://doi.org/10.1021/ja3066978.

[15] J.L. Fiorio, N. López, L.M. Rossi, Gold-Ligand-Catalyzed Selective Hydrogenation of Alkynes into cis-Alkenes via H2 Heterolytic Activation by Frustrated Lewis Pairs, ACS Catal. 7 (2017) 2973–2980. https://doi.org/10.1021/acscatal.6b03441.

[16] M. Stratakis, H. Garcia, Catalysis by supported gold nanoparticles: Beyond aerobic oxidative processes, Chem. Rev. 112 (2012) 4469–4506. https://doi.org/10.1021/cr3000785.

[17] A. Wittstock, M. Bäumer, Catalysis by unsupported skeletal gold catalysts, Acc. Chem. Res. 47 (2014) 731–739. https://doi.org/10.1021/ar400202p.

[18] R. Ciriminna, E. Falletta, C. Della Pina, J.H. Teles, M. Pagliaro, Industrial Applications of Gold Catalysis, Angew. Chemie - Int. Ed. 55 (2016) 14210–14217. https://doi.org/10.1002/anie.201604656.

[19] M. Yan, T. Jin, Y. Ishikawa, T. Minato, T. Fujita, L.Y. Chen, M. Bao, N. Asao, M.W. Chen, Y. Yamamoto, Nanoporous gold catalyst for highly selective semihydrogenation of alkynes: Remarkable effect of amine additives, J. Am. Chem. Soc. 134 (2012) 17536–17542. https://doi.org/10.1021/ja3087592.

[20] L. Liu, A. Corma, Metal Catalysts for Heterogeneous Catalysis: From Single Atoms to Nanoclusters and Nanoparticles, Chem. Rev. 118 (2018) 4981–5079. https://doi.org/10.1021/acs.chemrev.7b00776.

[21] Y. Zhu, H. Qian, B.A. Drake, R. Jin, Atomically Precise Au 25 (SR) 18 Nanoparticles as Catalysts for the Selective Hydrogenation of α,β-Unsaturated Ketones and Aldehydes , Angew. Chemie. 122 (2010) 1317–1320. https://doi.org/10.1002/ange.200906249.

[22] A. Shivhare, S.J. Ambrose, H. Zhang, R.W. Purves, R.W.J. Scott, Stable and

recyclable Au25 clusters for the reduction of 4-nitrophenol, Chem. Commun. 49 (2013) 276–278. https://doi.org/10.1039/c2cc37205c.

[23] H. Yamamoto, H. Yano, H. Kouchi, Y. Obora, R. Arakawa, H. Kawasaki, N,N-Dimethylformamide-stabilized gold nanoclusters as a catalyst for the reduction of 4-nitrophenol, Nanoscale. 4 (2012) 4148–4154. https://doi.org/10.1039/c2nr30222e.

[24] G. Li, C. Zeng, R. Jin, Thermally robust Au99(SPh)42 nanoclusters for chemoselective hydrogenation of nitrobenzaldehyde derivatives in water, J. Am. Chem. Soc. 136 (2014) 3673–3679. https://doi.org/10.1021/ja500121v.

[25] G. Li, R. Jin, Gold nanocluster-catalyzed semihydrogenation: A unique activation pathway for terminal alkynes, J. Am. Chem. Soc. 136 (2014) 11347–11354. https://doi.org/10.1021/ja503724j.

[26] P. Anastas, N. Eghbali, Green Chemistry: Principles and Practice, Chem. Soc. Rev. 39 (2010) 301–312. https://doi.org/10.1039/b918763b.

[27] J. Zhao, L. Ge, H. Yuan, Y. Liu, Y. Gui, B. Zhang, L. Zhou, S. Fang, Heterogeneous gold catalysts for selective hydrogenation: From nanoparticles to atomically precise nanoclusters, Nanoscale. 11 (2019) 11429–11436. https://doi.org/10.1039/c9nr03182k.

[28] A.E. Palomares, C. Franch, A. Corma, A study of different supports for the catalytic reduction of nitrates from natural water with a continuous reactor, Catal. Today. 172 (2011) 90–94. https://doi.org/10.1016/j.cattod.2011.05.015.

[29] V. Truttmann, C. Herzig, I. Illes, A. Limbeck, E. Pittenauer, M. Stöger-Pollach, G. Allmaier, T. Bürgi, N. Barrabés, G. Rupprechter, Ligand engineering of immobilized nanoclusters on surfaces: Ligand exchange reactions with supported Au11(PPh3)7Br3, Nanoscale. 12 (2020) 12809–12816. https://doi.org/10.1039/c9nr10353h.

[30] J.K. Bartley, C. Xu, R. Lloyd, D.I. Enache, D.W. Knight, G.J. Hutchings, Simple method to synthesize high surface area magnesium oxide and its use as a heterogeneous base catalyst, Appl. Catal. B Environ. 128 (2012) 31–38. https://doi.org/10.1016/j.apcatb.2012.03.036.

[31] X.-K. Wan, J.-Q. Wang, Z.-A. Nan, Q.-M. Wang, Ligand effects in catalysis by atomically precise gold nanoclusters, Sci. Adv. 3 (2017) e1701823. https://doi.org/10.3866/PKU.WHXB201710301.

[32] I. López-Hernández, C. García, V. Truttmann, S. Pollitt, N. Barrabés, G. Rupprechter, F. Rey, A.E. Palomares, Evaluation of the silver species nature in Ag-ITQ2 zeolites by the CO oxidation reaction, Catal. Today. 345 (2020) 22–26. https://doi.org/10.1016/j.cattod.2019.12.001.

[33] C.P. Joshi, M.S. Bootharaju, M.J. Alhilaly, O.M. Bakr, [Ag25(SR)18]-: The “golden”Silver Nanoparticle Silver Nanoparticle, J. Am. Chem. Soc. 137 (2015) 11578–11581. https://doi.org/10.1021/jacs.5b07088.

[34] Y. Liu, H. Tsunoyama, T. Akita, T. Tsukuda, Preparation of ∼1 nm Gold Clusters Confined within Mesoporous Silica and Microwave-Assisted Catalytic Application for Alcohol Oxidation, J. Phys. Chem. C. 113 (2009) 13457–13461. https://doi.org/10.1021/jp904700p.

[35] A. Noujima, T. Mitsudome, T. Mizugaki, K. Jitsukawa, K. Kaneda, Unique catalysis of gold nanoparticles in the chemoselective hydrogenolysis with H2: Cooperative effect between small gold nanoparticles and a basic support, Chem. Commun. 48 (2012) 6723–6725. https://doi.org/10.1039/c2cc32850j.

[36] L. Shao, X. Huang, D. Teschner, W. Zhang, Gold supported on graphene oxide: An active and selective catalyst for phenylacetylene hydrogenations at low temperatures, ACS Catal. 4 (2014) 2369–2373. https://doi.org/10.1021/cs5002724.

[37] C. García, S. Pollitt, M. van der Linden, V. Truttmann, C. Rameshan, R. Rameshan, E. Pittenauer, G. Allmaier, P. Kregsamer, M. Stöger-Pollach, N. Barrabés, G. Rupprechter, Support effect on the reactivity and stability of Au25(SR)18 and Au144(SR)60 nanoclusters in liquid phase cyclohexane oxidation, Catal. Today. 336 (2019) 174–185. https://doi.org/10.1016/j.cattod.2018.12.013.

[38] B. Zhang, C. García, A. Sels, G. Salassa, C. Rameshan, J. Llorca, K. Hradil, G. Rupprechter, N. Barrabés, T. Bürgi, Ligand and support effects on the reactivity and stability of Au38(SR)24 catalysts in oxidation reactions, Catal. Commun.

130 (2019) 105768. https://doi.org/10.1016/j.catcom.2019.105768.

[39] A. Ayala, G. Fetter, E. Palomares, P. Bosch, CuNi/Al hydrotalcites synthesized in presence of microwave irradiation, Mater. Lett. 65 (2011) 1663–1665. https://doi.org/10.1016/j.matlet.2011.03.004.

[40] N. Blanch-Raga, A.E. Palomares, J. Martínez-Triguero, G. Fetter, P. Bosch, Cu mixed oxides based on hydrotalcite-like compounds for the oxidation of trichloroethylene, Ind. Eng. Chem. Res. 52 (2013) 15772–15779. https://doi.org/10.1021/ie4024935.

[41] N. Blanch-Raga, A.E. Palomares, J. Martínez-Triguero, M. Puche, G. Fetter, P. Bosch, The oxidation of trichloroethylene over different mixed oxides derived from hydrotalcites, Appl. Catal. B Environ. 160–161 (2014) 129–134. https://doi.org/10.1016/j.apcatb.2014.05.014.

[42] A. Noujima, T. Mitsudome, T. Mizugaki, K. Jitsukawa, K. Kaneda, Selective deoxygenation of epoxides to alkenes with molecular hydrogen using a hydrotalcite-supported gold catalyst: Aconcerted effect between gold nanoparticles and basic sites on a support, Angew. Chemie - Int. Ed. 50 (2011) 2986–2989. https://doi.org/10.1002/anie.201007679.

[43] T. Mitsudome, A. Noujima, Y. Mikami, T. Mizugaki, K. Jitsukawa, K. Kaneda, Supported gold and silver nanoparticles for catalytic deoxygenation of epoxides into alkenes, Angew. Chemie - Int. Ed. 49 (2010) 5545–5548. https://doi.org/10.1002/anie.201001055.

CAPTION TO FIGURES

Figure 1. Activity of fresh nanoclusters with different size (Au_{11} and Au_{25}) supported on alumina and magnesia for the phenylacetylene semihydrogenation (0.1 g. of catalyst, 0.1 mmol of phenylacetylene and 0.2 mmol of pyridine, 100 ºC, 10 bar of H_2). (🟩) conversion, (🟦) selectivity towards styrene, (🟧) selectivity towards ethylbenzene.

Figure 2. Activity of the Au_{11}/Al_2O_3 catalysts pretreated with air (Au_{11}Al_oxi) or with hydrogen (Au_{11}Al_red) for the phenylacetylene semihydrogenation (0.1 g. of catalyst, 0.1 mmol of phenylacetylene and 0.2 mmol of pyridine, 100 ºC, 10 bar of H_2). (🟩) conversion, (🟦) selectivity towards styrene, (🟧) selectivity towards ethylbenzene.

Figure 3. UV-Vis DRS spectra of the Au_{11}/Al_2O_3 catalyst before (_fresh) and after reductive (_red) and oxidative (_oxi) pretreatments.

Figure 4. Activity of gold nanoclusters supported on alumina and magnesia and pretreated with H_2 for the phenylacetylene semihydrogenation (0.1 g. of catalyst, 0.1 mmol of phenylacetylene and 0.2 mmol of pyridine, 100 ºC, 10 bar of H_2). (🟩) conversion, (🟦) selectivity towards styrene, (🟧) selectivity towards ethylbenzene.

Figure 5. UV-Vis DRS spectra of the Au_{11} and Au_{25} catalysts supported on MgO after reductive pretreatment.

Figure 6. Phenylacetylene semihydrogenation reaction over Au_{25} pre-reduced catalysts supported on MgO (Au_{25}Mg_red), Al_2O_3 (Au_{25}Al_red) and Mg/Al hydrotalcite (Au_{25}HT_red) (0.1 g. of catalyst, 0.1 mmol of phenylacetylene and 0.2 mmol of pyridine, 100 ºC, 10 bar H_2). (🟩) conversion, (🟦) selectivity towards styrene, (🟧) selectivity towards ethylbenzene.

Figure 7. Infrared spectra of pyridine desorption at 150ºC, 250ºC and 350ºC of the Au_{25} catalysts supported on MgO, Al_2O_3 and hydrotalcite and pretreated with H_2.

Figure 8. TPR profiles of the pre-oxidized Au_{25} catalysts supported on MgO, Al_2O_3 and hydrotalcite.

Supporting Information

Gold nanoclusters supported on different materials as catalysts for the selective alkyne semihydrogenation

I. López-Hernández[1], V. Truttmann[2], N. Barrabés[2,*], G. Rupprechter[2], F. Rey[1], J. Mengual[1], A. E. Palomares[1,*]
[1]Instituto de Tecnología Química, Universitat Politècnica de València - Consejo Superior de Investigaciones Científicas (UPV-CSIC), Valencia, España
[2]Institute of Materials Chemistry, TU Wien, Vienna, Austria

Corresponding author: apalomar@iqn.upv.es, noelia.rabanal@tuwien.ac.at

Characterization Techniques

X-ray powder diffraction (XRD) was carried out using a Philips X'Pert (Cubix-Pro)-advance diffractometer operating at 45 kV and 40 mA, and coupled to a copper anode X-ray tube (Cu Kα radiation, λ = 1.542 Å).

UV-Vis spectra of nanoclusters dissolved in CH_2Cl_2 were recorded on a Perkin Elmer Lambda 750 UV-Vis spectrometer.

Blank reactions

A blank reaction was made without adding catalysts observing that in these conditions no conversion was obtained.

Experiments with the supports without adding gold were also made obtaining in all cases conversions lower than 15%

XRD characterization of supports

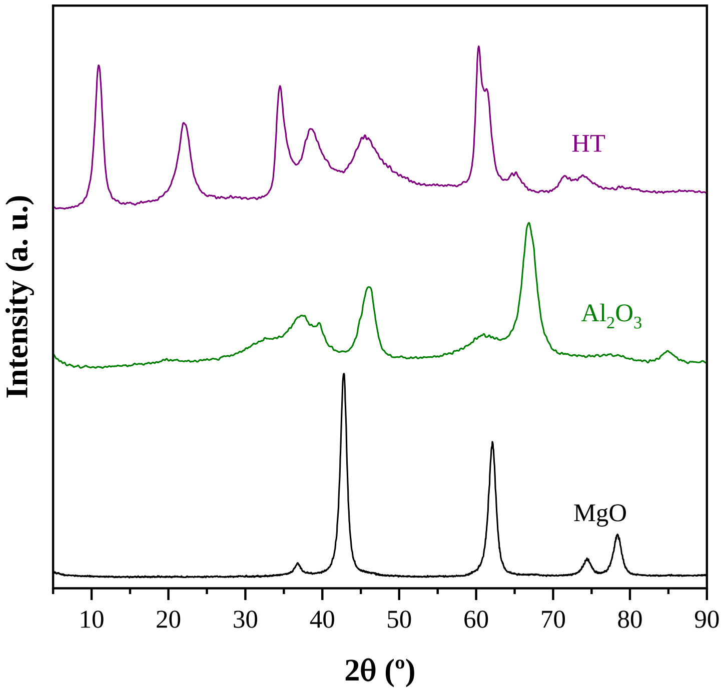

Figure S1. XRD patterns of the supports.

UV-Vis spectra of the nanocluster samples in solution

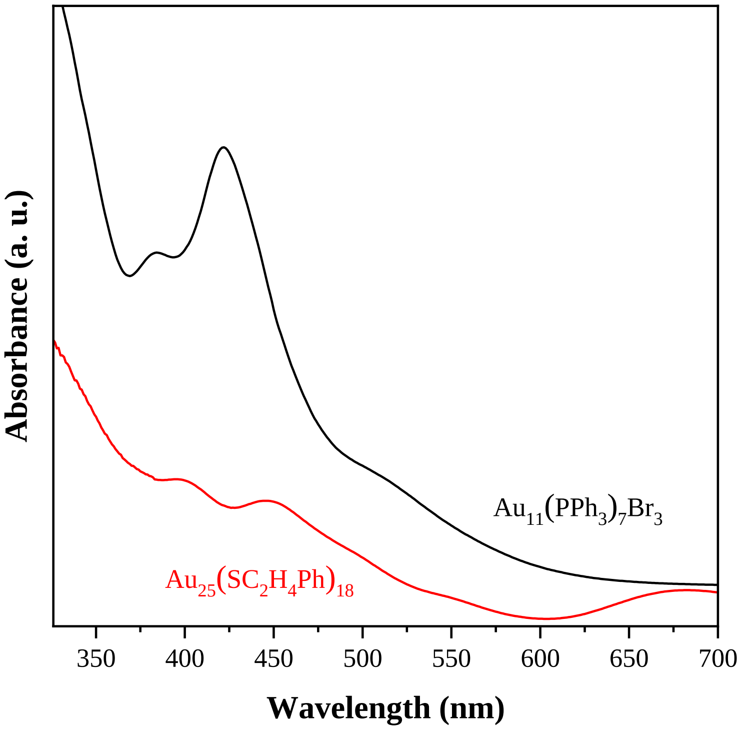

Figure S2. UV-Vis spectra of synthetized Au_{11} and Au_{25} nanoclusters.

Table 1: Surface area and chemical composition of the catalysts.

Catalyst	**S_{BET} (m^2 g^{-1})**	**Au (wt.%)**
Au_{11}/Al_2O_3	199	0.44
Au_{11}/MgO	107	0.30
Au_{25}/Al_2O_3	202	0.17
Au_{25}/MgO	121	0.19
Au_{25}/Hydrotalcite (molar ratio Mg/Al = 4)	224	0.06

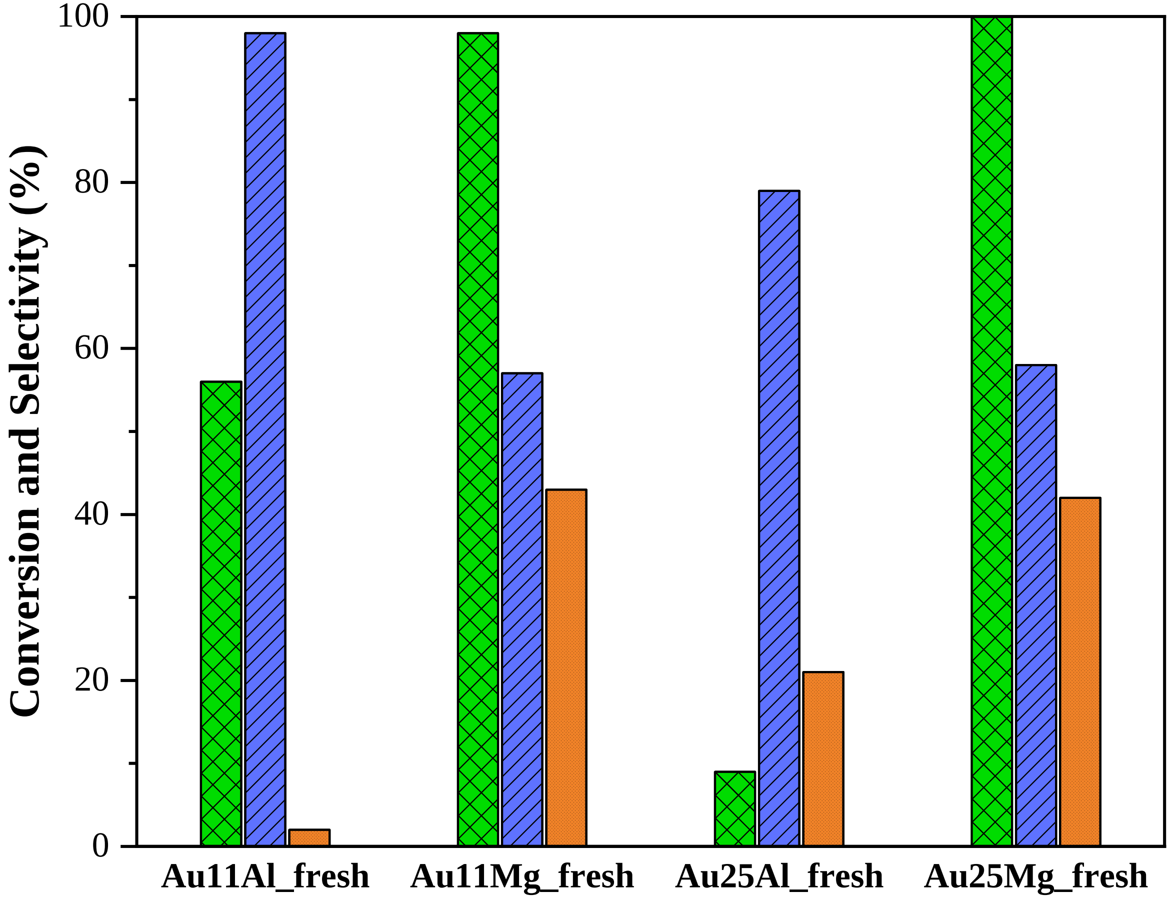
Conversion and Selectivity (%)
0
20
40
60
80
100
Au11Al_fresh
Au11Mg_fresh
Au25Al_fresh
Au25Mg_fresh

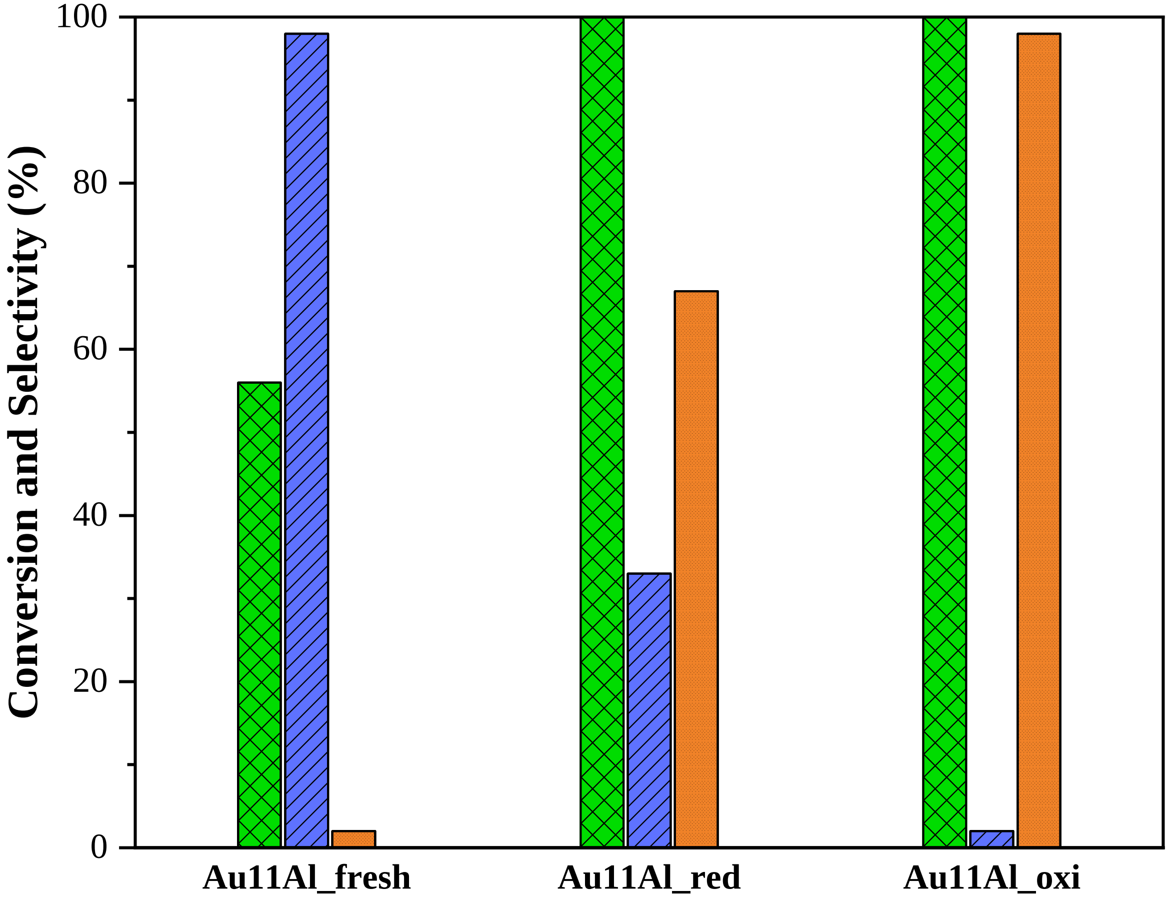
Conversion and Selectivity (%)
0
20
40
60
80
100
Au11Al_fresh
Au11Al_red
Au11Al_oxi

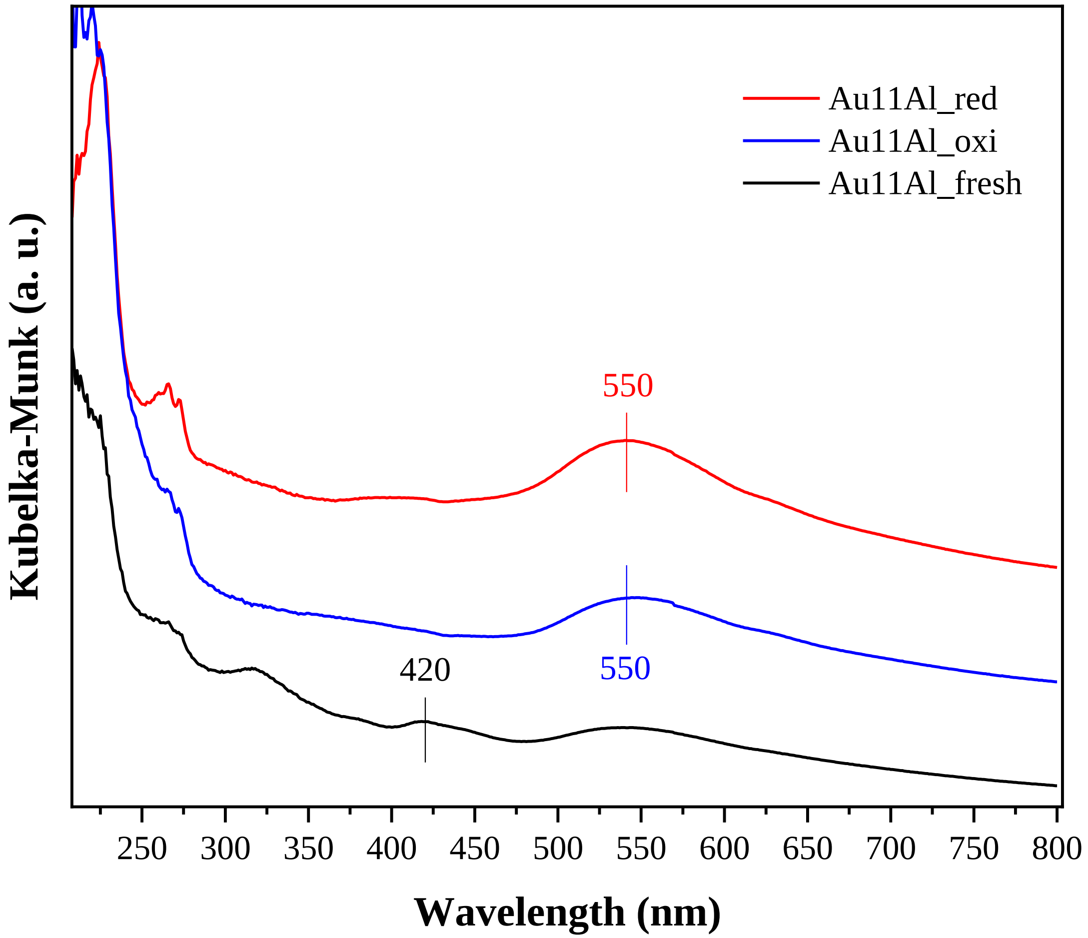
Au11Al_red
Au11Al_oxi
Au11Al_fresh
550
550
420
Kubelka-Munk (a. u.)
250
300
350
400
450
500
550
600
650
700
750
800
Wavelength (nm)

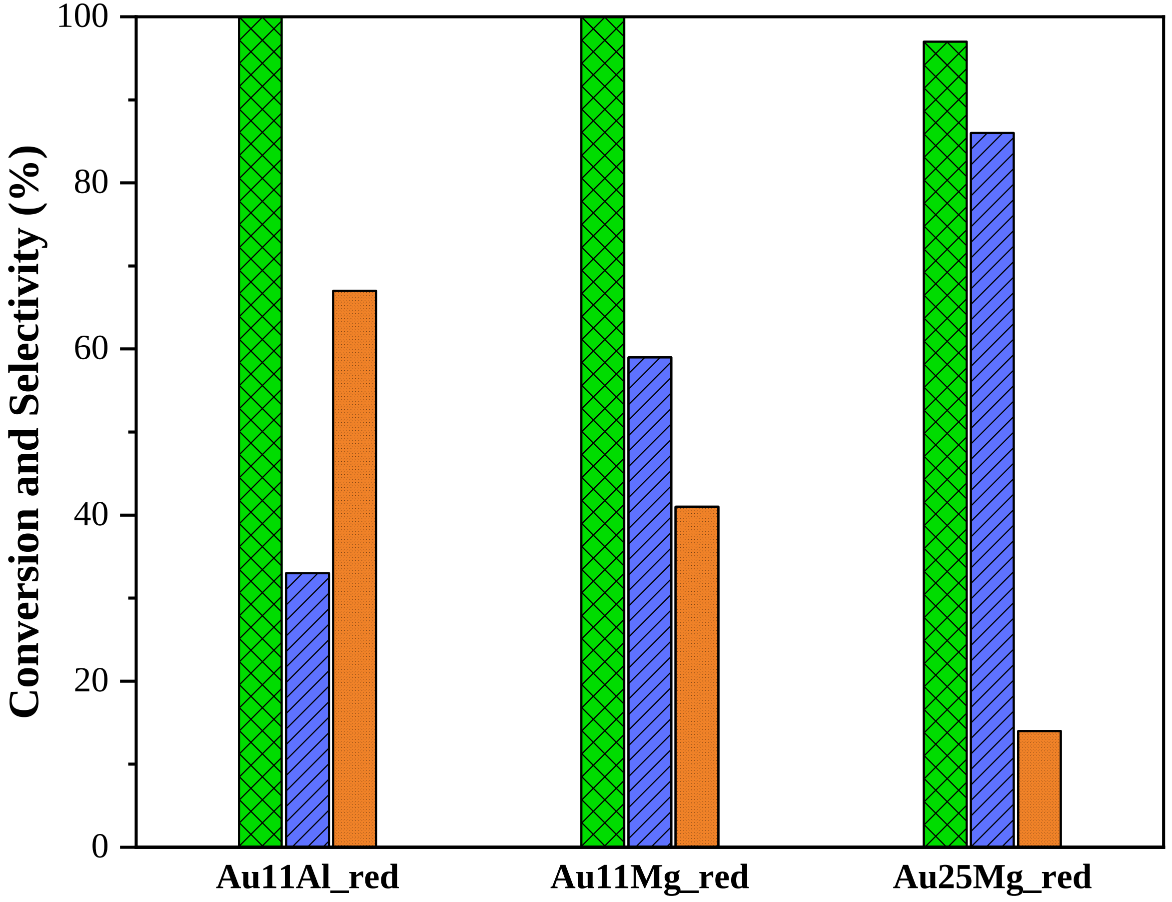
Conversion and Selectivity (%)
100
80
60
40
20
0
Au11Al_red
Au11Mg_red
Au25Mg_red

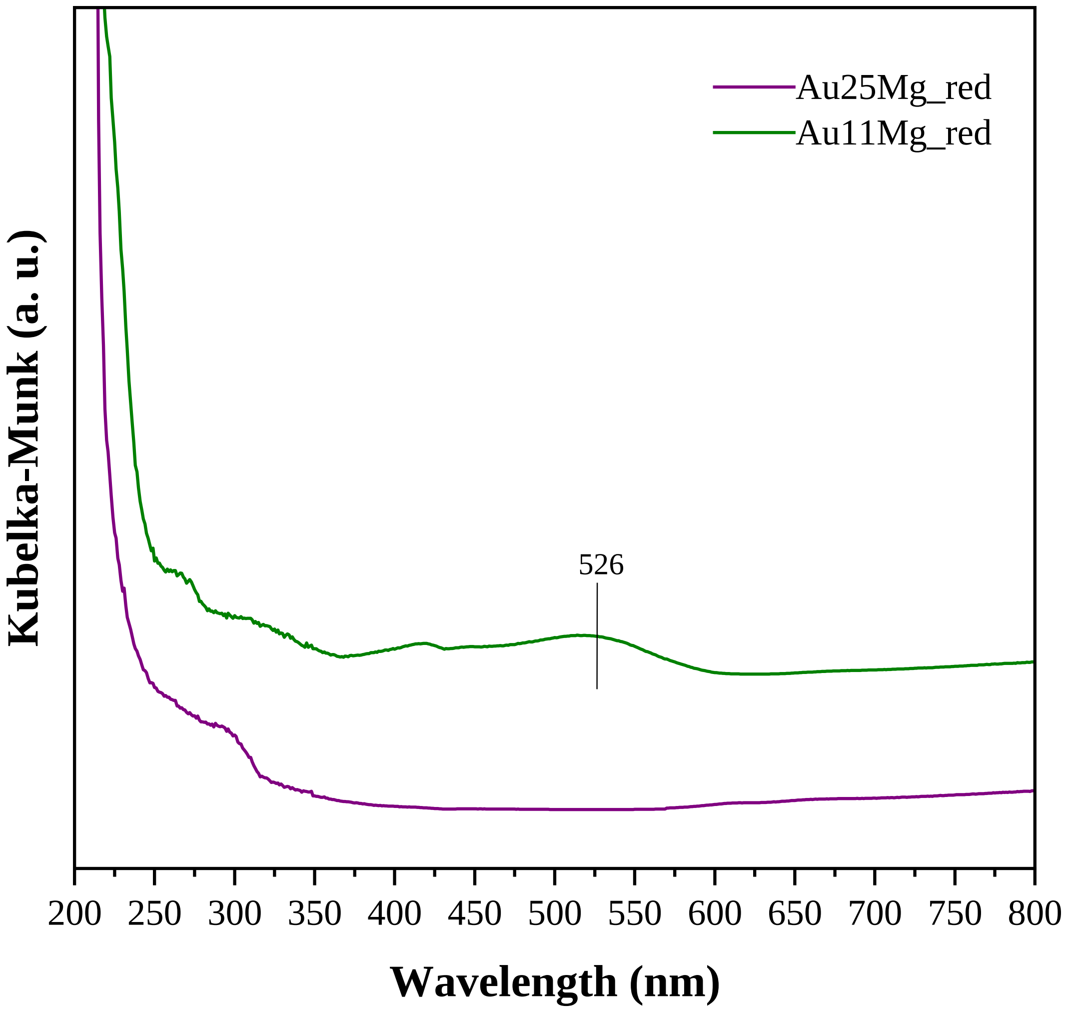
Au25Mg_red
Au11Mg_red
526
Kubelka-Munk (a. u.)
Wavelength (nm)
200
250
300
350
400
450
500
550
600
650
700
750
800

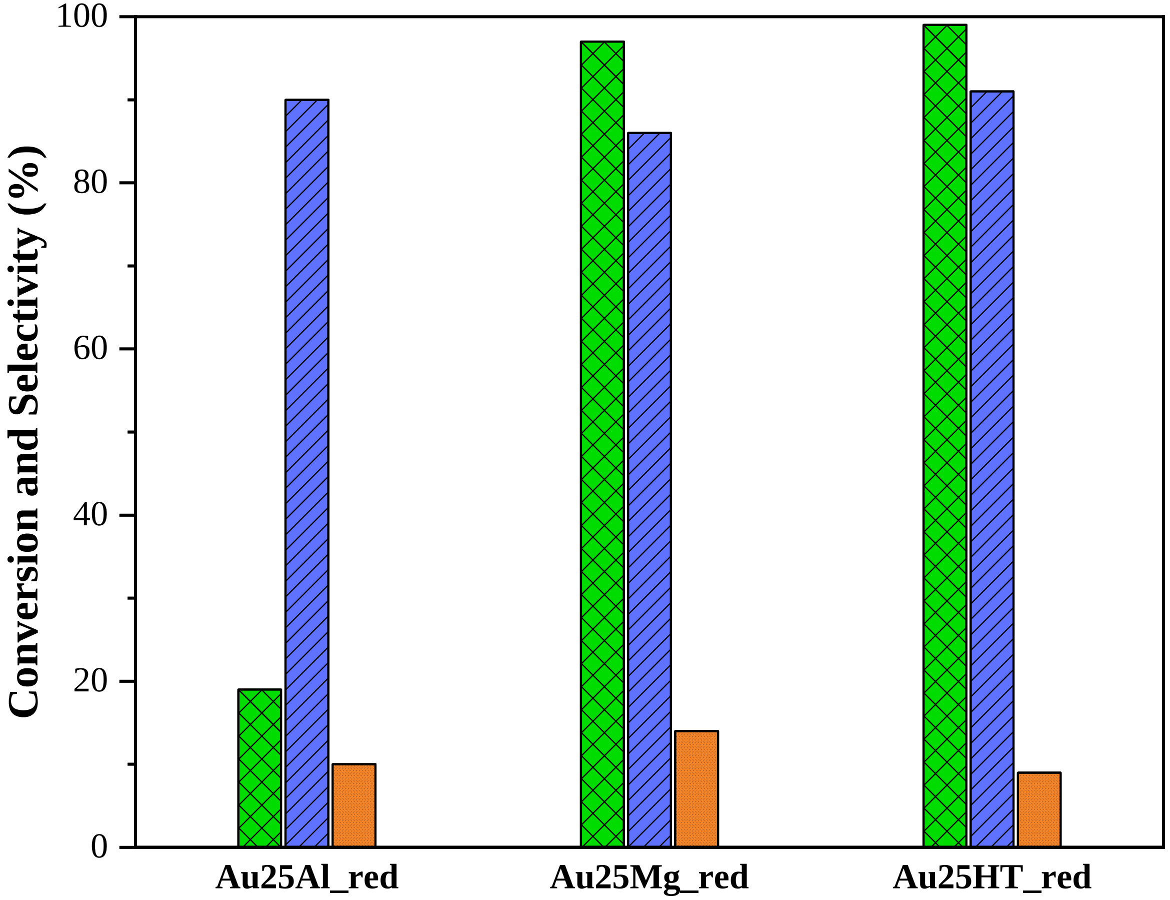
Conversion and Selectivity (%)
100
80
60
40
20
0
Au25Al_red
Au25Mg_red
Au25HT_red

Figure 7

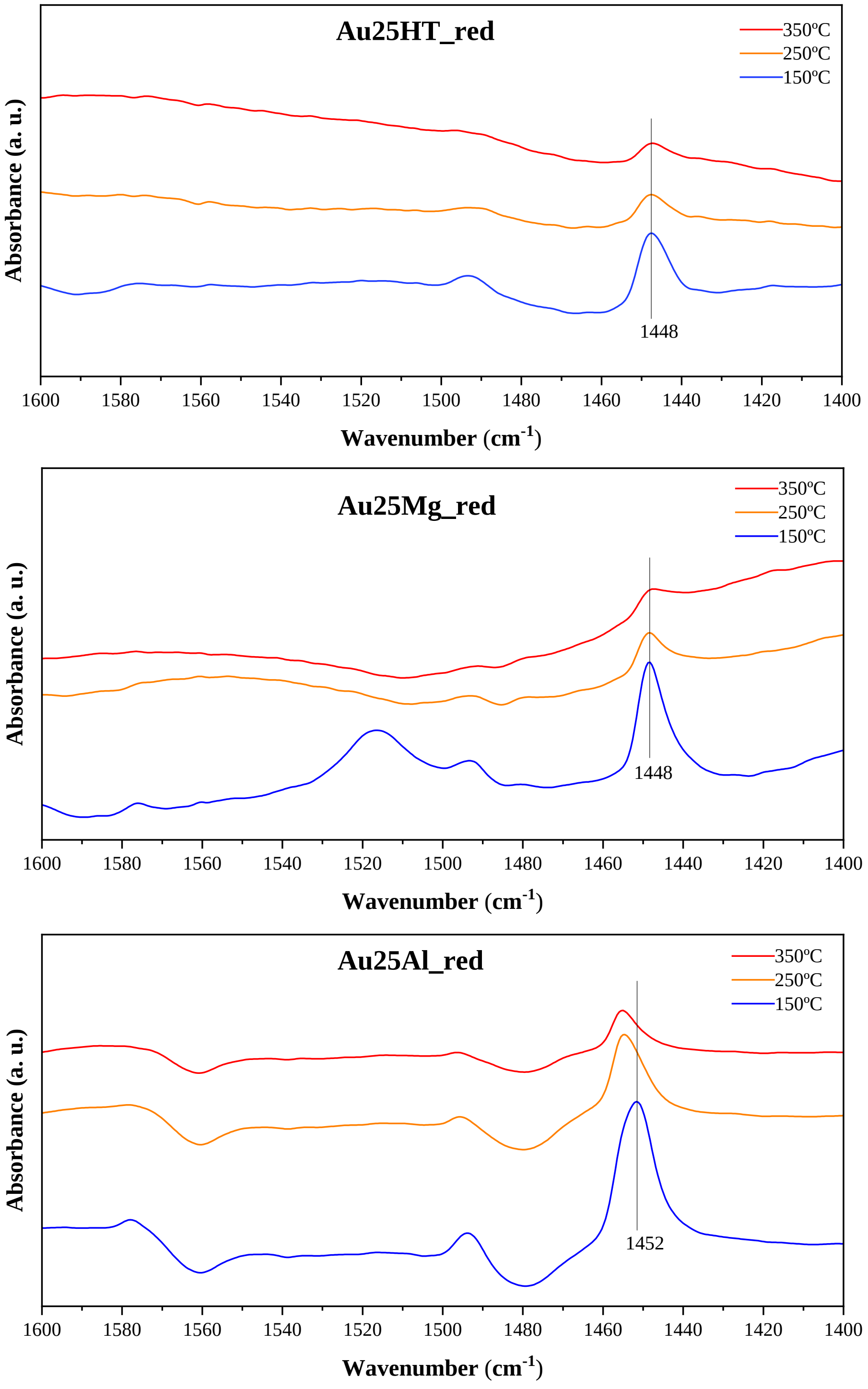
Au25HT_red
350ºC
250ºC
150ºC
1448
Absorbance (a. u.)
1600
1580
1560
1540
1520
1500
1480
1460
1440
1420
1400
Wavenumber (cm-1)
Au25Mg_red
350ºC
250ºC
150ºC
1448
Absorbance (a. u.)
1600
1580
1560
1540
1520
1500
1480
1460
1440
1420
1400
Wavenumber (cm-1)
Au25Al_red
350ºC
250ºC
150ºC
1452
Absorbance (a. u.)
1600
1580
1560
1540
1520
1500
1480
1460
1440
1420
1400
Wavenumber (cm-1)

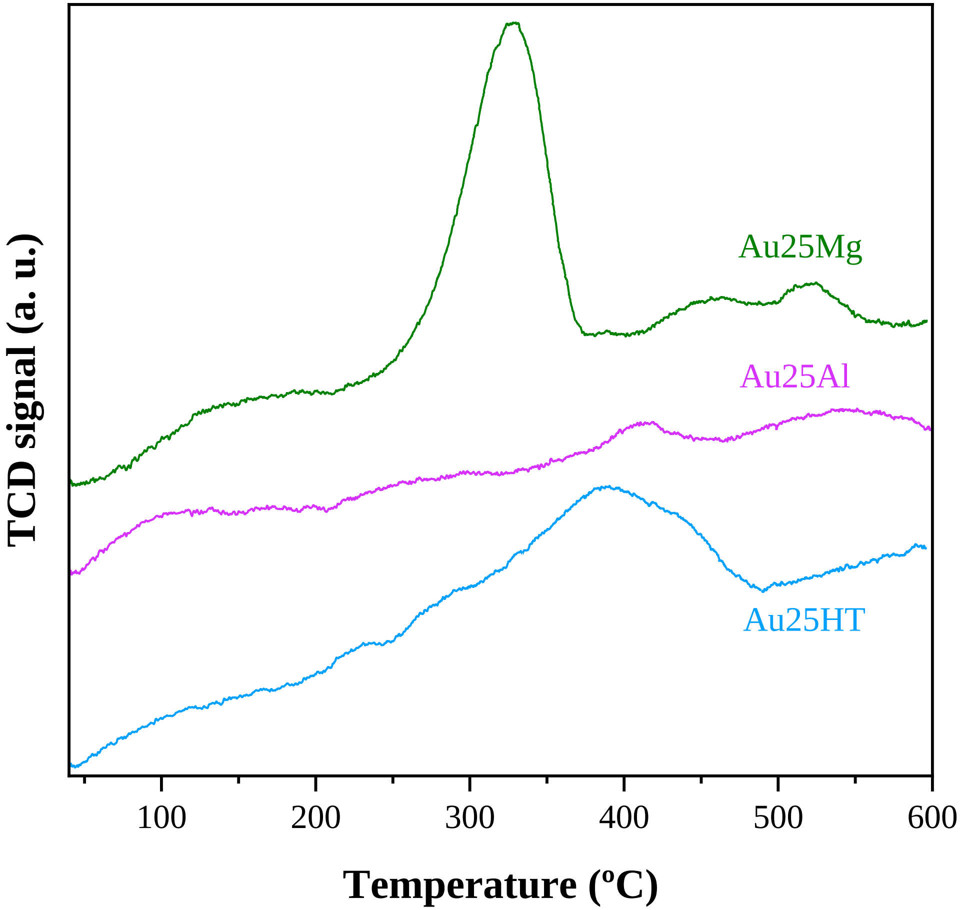
Au25Mg
Au25Al
Au25HT
TCD signal (a. u.)
100
200
300
400
500
600
Temperature (ºC)

Declaration of interests

☒ The authors declare that they have no known competing financial interests or personal relationships that could have appeared to influence the work reported in this paper.

☐The authors declare the following financial interests/personal relationships which may be considered as potential competing interests: